International Journal of Refrigeration 123 (2021) 138–149

Contents lists available at ScienceDirect

International Journal of Refrigeration

journal homepage: www.elsevier.com/locate/ijrefrig

CFD analysis for predicting cooling time of a domestic refrigerator with thermoelectric cooling system

Engin Söylemez[a,*], Emre Alpman[b], Ayhan Onat[c], Selim Hartomacıoğlu[c]

[a] NTNU, Department of Energy and Process Engineering, Process and Power Research Group, Trondheim, Norway
[b] Marmara University, Department of Mechanical Engineering, Faculty of Engineering, Istanbul, Turkey
[c] Marmara University, Department of Mechanical Engineering, Faculty of Technology, Istanbul, Turkey

ARTICLE INFO

Article history:
Received 18 May 2020
Revised 17 November 2020
Accepted 20 November 2020
Available online 26 November 2020

Keywords:
CFD analysis
Cooling time
Fresh food
Domestic refrigerator
Thermoelectric cooler
Vapour compression

ABSTRACT

In this work, Computational Fluid Dynamics (CFD) analysis was conducted considering three different turbulence (viscous) models for a fresh food compartment of a domestic refrigerator (DR), in order to not only gain idea on cooling down time rate of fresh food compartment but also present air and temperature distribution inside the compartment when it is loaded. The refrigerator composes of three compartments: Fresh food (FFC), chill (CC) and freezer (FC). The FFC compartment is cooled by a thermoelectric/Peltier cooler (TEC) while the other compartments are handled by a vapour compression (VC) system. To measure cooling times, tests were conducted according to new IEC62552:2015 standard in climatic chambers and the cooling time was measured as 146.5 min. The predictions of developed CFD model clearly visualize the airflow and temperature fields inside the FFC. Concerning numerical predictions for the packages in the upper regions were in better agreement (below 10%) with measurements than the predictions for the packages in the lower regions mainly due to convective heat transfer behaviour.

© 2020 The Author(s). Published by Elsevier Ltd.
This is an open access article under the CC BY license (http://creativecommons.org/licenses/by/4.0/)

Analyse CFD pour la prévision de la durée de refroidissement d'un réfrigérateur domestique avec système de refroidissement thermoélectrique

Mots-clés: Analyse CFD; Durée de refroidissement; Produits frais; Réfrigérateur domestique; Refroidisseur thermoélectrique; Compression de vapeur

1. Introduction

Preserving foods' nutritional values at low temperatures for a longer storage time is critical in domestic refrigerators. Bringing foods to low temperature levels by means of cooling and freezing processes decreases the microorganisms' (bacteria, yeasts, molds, and viruses) activities that accelerate the food deterioration (ASHRAE, 2014). The foods shall be stored at more optimum conditions. This becomes more critical for the fresh food compartment (FFC) in which more perishable foods are held. To have more optimum preservation conditions, the most important method is to improve the uniformity of temperature distribution inside the compartments of refrigerators (Ding et al., 2004). However, it cannot always be thoroughly possible to get the same temperature levels at all locations in the compartments. Temperature stratification is inevitable due to the, (1) height of the compartment (the cold air tends to move down to the bottom) (2) on-off operation of cooling system (3) variations in heat leakages in different parts of the compartment (the heat transfer rates may vary through walls and door gaskets) (4) design of air flow system (air near the delivery channels is colder than the one near the return channels) (Fukuyo et al., 2003; Ding et al., 2004). Yet, this can be an advantage if the end-users are informed by the manufacturers about ideal storing conditions for each foodstuff.

In addition to the temperature uniformity, it is key to effectively cool down the warm foods as fast as possible to the required tem-

* Corresponding author.
E-mail address: engin.soylemez@ntnu.no (E. Söylemez).

https://doi.org/10.1016/j.ijrefrig.2020.11.012
0140-7007/© 2020 The Author(s). Published by Elsevier Ltd. This is an open access article under the CC BY license (http://creativecommons.org/licenses/by/4.0/)

Nomenclature

Abbreviations

CC	Chill compartment
CFD	Computational fluid dynamics
Cu	Copper
DC	Direct current (A)
DR	Domestic refrigerator
FC	Freezer compartment
FFC	Fresh food compartment
IEC	International Electrotechnical Commission
Ma	Mach number
TE	Thermoelectric
TEC	Thermoelectric cooler
VC	Vapour compression

Symbols

A_s	Surface area (m^2)
D	Depth (mm)
c_p	Specific heat at constant pressure ($kJkg^{-1}\ ^\circ C^{-1}$)
g	Gravitational acceleration (9.81 ms^{-2})
Gr_L	Grashof number
h	Convection heat transfer coefficient ($Wm^{-2}K^{-1}$)
H	Height (mm)
k	Effective thermal conductivity ($Wm^{-1}K^{-1}$)
L	Length (m)
L_c	Characteristic length (m)
m	Mass (kg)
Nu	Nusselt number
p	Static pressure (Pa)
P_s	Perimeter of the surface (m)
Pr	Prandtl number
Ra_L	Rayleigh number
t	Time (s)
T	Temperature (K)
T_a	Ambient temperature (K)
T_s	Temperature of outer surfaces (K)
T_∞	Temperature of air sufficiently away from the surface (K)
V	Velocity vector (ms^{-1})
∇	Gradient operator
W	Width (mm)

Greek symbols

β	Coefficient of volume expansion (K^{-1})
ρ	Density (kgm^{-3})
μ	Effective viscosity (Pa s)
Φ	Viscous-dissipation function
ν	Effective kinematic viscosity of the air (m^2s^{-1})

perature levels (below 10 °C) in order to slow down decay in foods (ASHRAE, 2014; Fukuyo et al., 2003).

There have been several studies considering airflow and temperature distribution in the DRs. António & Afonso (2011) monitored temperatures inside a DR. They measured temperatures and compared the measuremt results with the ones predicted by the Fluent code and Artificial Neural Network and concluded that in their case the Artificial Neural Network predicted a lower absolute error compared to CFD's predictions (António and Afonso, 2011). In another work, Belman-Flores & Gallegos-Muñoz (2016) analysed the air flow and thermal behaviour of the compartment in a refrigerator by means of CFD to compare the effect of two different evaporators on flow and temperature distribution (Belman-Flores and Gallegos-Muñoz, 2016). They claimed the CFD as a feasible tool for evaluating of internal design of the refrigerator. Belman-Flores et al. (2014) proposed a new design for the FFC of a DR so as to improve temperature distribution in the compartment. They used CFD tool for predictions and achieved more uniform temperature distribution in the FFC compared with that of original FFC design (Belman-Flores et al., 2014). Bayer et al. (2013) simulated the fluid flow and temperature distribution in a commercial refrigerator compartment through CFD tool. Their study presented that the radiation does not have a significant effect on the temperature distribution in the compartment although it has a considerable effect on the heat rates (Bayer et al., 2013). Zhang & Lian (2014) conducted a numerical study on the air circulation and heat transfer in an DR. Three refrigerator configurations were analysed to understand the effect of inner structure on the air velocity and temperature distribution and heat loss of the refrigerators. It was concluded that vertical temperature stratification was seen in the FFC of all configurations (Zhang and Lian, 2014). Gupta et al. (2007) developed a CFD model for a domestic frost-free refrigerator in order to predict air velocity and temperature distribution inside the FFC and FC. The CFD predictions and experimental results were in good agreement in their study (Gupta et al., 2007). Nikitin (2020) conducted a simulation analysis by using OpenFOAM with open refrigerated display cabinets. The design solutions for the display cabinets were proposed and their suitability were proved (Nikitin, 2020). Ding et al. (2004) performed a numerical and experimental investigation to improve temperature uniformity inside a refrigerator. They proposed a new inner design and cooling chamber for the refrigerator and then proved that the temperature field in the new design is more uniform than that of the original refrigerator (Ding et al., 2004). Alfaro-Ayala et al. (2017) predicted temperature and air velocity distribution in a cooling cabinet through CFD analysis by using three different models. They recommended the most appropriate approaches for the prediction of temperature distribution at unsteady conditions (Alfaro-Ayala et al., 2017). In these studies, the investigated appliances had mostly VC system and were empty.

Fukuyo et al. (2003) developed a new air-supply system to improve temperature uniformity and cooling rate inside an FFC of a household refrigerator (Fukuyo et al., 2003). They introduced a blower and jet slots to a cooled air supply system. They achieved not only more uniform temperature distribution but also a four times higher cooling rate. Laguerre et al. (2007) studied airflow and heat transfer by natural convection inside the fridge compartment of a static type domestic refrigerator. They considered three configurations: an empty refrigerator with and without shelves, and refrigerator loaded with packages. They developed CFD simulation model and it is demonstrated that CFD predictions for air temperatures inside the fridge are in good agreement when radiation effects are taken into consideration (Laguerre et al., 2007). Laguerre et al. (2009) investigated the combined effect of heat, moisture transport, and airflow by natural convection in a rectangular cavity with online cylinders/obstacles. In the experimental part of their work, temperature, velocity and humidity fields on the symmetry plane at steady state conditions were measured in unhumidified and humidified cavity. Then, numerical work was performed through CFD simulation and measurement results were compared with the CFD predictions. They observe the thermal stratification and circular airflow in the cavity (Laguerre et al., 2009). In the following numerical work of Laguerre et al. (2010), evaporation and condensation phenomena because of natural convection in a domestic refrigerator without a fan were studied (Laguerre et al., 2010). They achieved to validate numerical methodology developed for the purpose of determining all possible locations of dehydration and condensation. Li et al. (2019) enhanced the temperature uniformity of a wine cooler. They first determined the factors that create temperature stratification inside the cabinet of the wine cooler, and then they

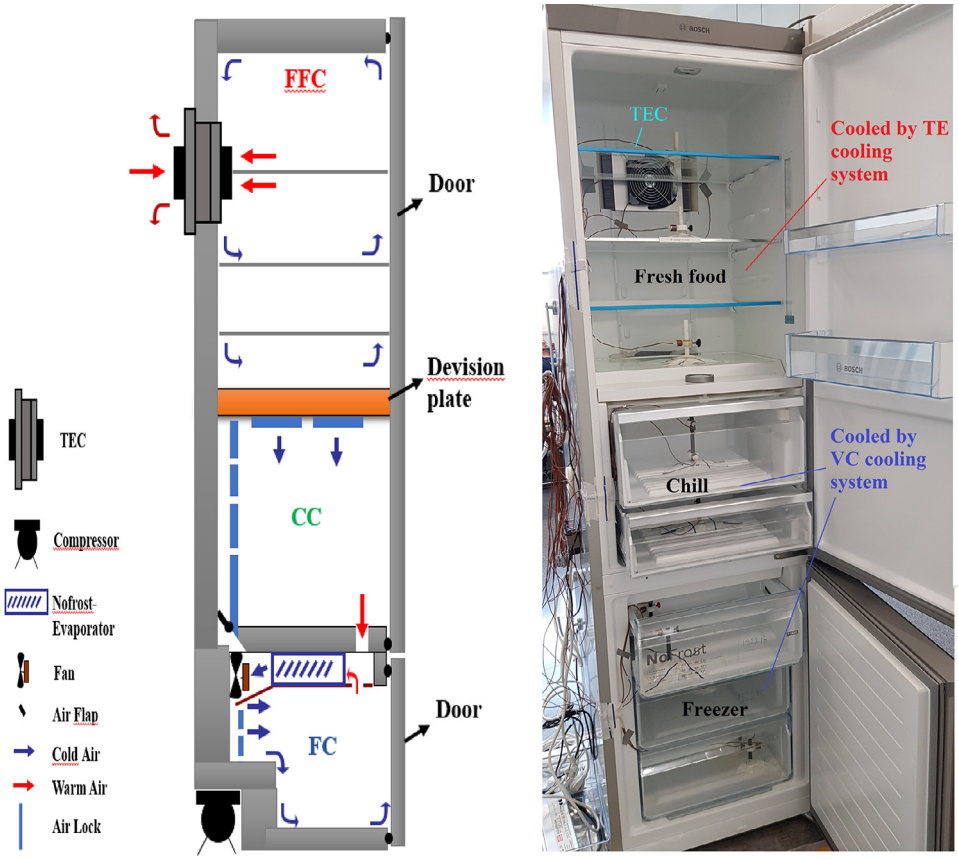


Fig. 1. The specifications and cooling systems of the tested refrigerator.

proposed four methods in order to eliminate temperature non-uniformity. When applying a combination of four methods, more uniformity in temperature was achieved in the cabinet and maximum temperature difference between the minimum and maximum temperature inside the cabinet was decreased from 12.1 °C to 1.9 °C (Li et al., 2019).

In the context of this work, the focus is given to the cooling time performance of FFC of a prototype TEC based domestic refrigerator. Similar prototype refrigerators have been used in the two previous works of the same Authors (Söylemez et al., 2018, 2019). In the first work, the effect of TEC on the cooling performance of the refrigerators was experimentally investigated. In the second work, the optimum location for TEC was determined via CFD predictions to achieve more uniform temperature and air velocity distribution inside the FFC.

As seen from the literature review above, there is no study that predicts the cooling time performance of a TEC-cooled fresh food compartment via CFD analysis and that refers to the tests conducted in accordance with the new IEC62552:2015 standard prepared for setting out new testing requirements for household refrigerating appliances. Based on this, in this experimental and numerical work, the goal is (1) to fill the existing scientific gap as regards the simulation studies of TEC-based refrigerators (2) to develop a simulation model by means of CFD tool in order to predict the cooling time for the FFC of a domestic refrigerator cooled by TEC (3) to verify the CFD predictions with the results of the measurements performed in conformity with the new standard. Unlike the earlier work (Söylemez et al., 2019); CFD analysis was conducted for the conditions of loaded and transient (unsteady). Flow was assumed fully turbulent and three different turbulence models were applied so as to find the most suitable one for the simulations. The models are standard k-ε, realizable k-ε, and transition SST.

2. Methodology

2.1. Importance of cooling time

There are in general two factors that inhibit the microbial growth: (1) intrinsic factors (nutrients, inhibitors, competing microorganisms, water activity, and pH) and (2) extrinsic factors (temperature, environmental relative humidity, and oxygen level) (ASHRAE, 2014). In the context of this work, the effect of temperature, which can be controlled by cooling, was under investigation.

The microbial growth is rapid when the foodstuffs are held in the environment temperatures of between 5 °C and 60 °C, which provides ideal conditions for pathogenic microorganisms, for more than 2 h (ASHRAE, 2014). Since the foodstuffs are usually in these temperature ranges before being inserted into the refrigerators, the time for lowering their temperatures from the environment temperature to the minimum growth temperature levels is crucial to extend their shelf life. It should be as fast as possible; because, the rapid cooling prevents the large crystallisation of water in food and therefore causes less damages in the cell membranes and in the tissue structure of the food. As a result, the microbial growth in the food is retarded that decreases enzymatic and respiratory activity and reduces moisture loss. Thus, spoilage is reduced, and the food's freshness and quality are prolonged.

2.2. Tested refrigerator

The analysed refrigerator is shown in Fig. 1. It has the compartments of fresh food (FFC), chill (CC), and freezer (FC). The TEC is applied to the FFC, while a compressor-based VC system is applied to CC and FC of the refrigerator. The TEC, CTA305, is an air-to-air exchanger, which is composed of P and N semiconductors connected in series along with aluminium fins to enhance heat trans-

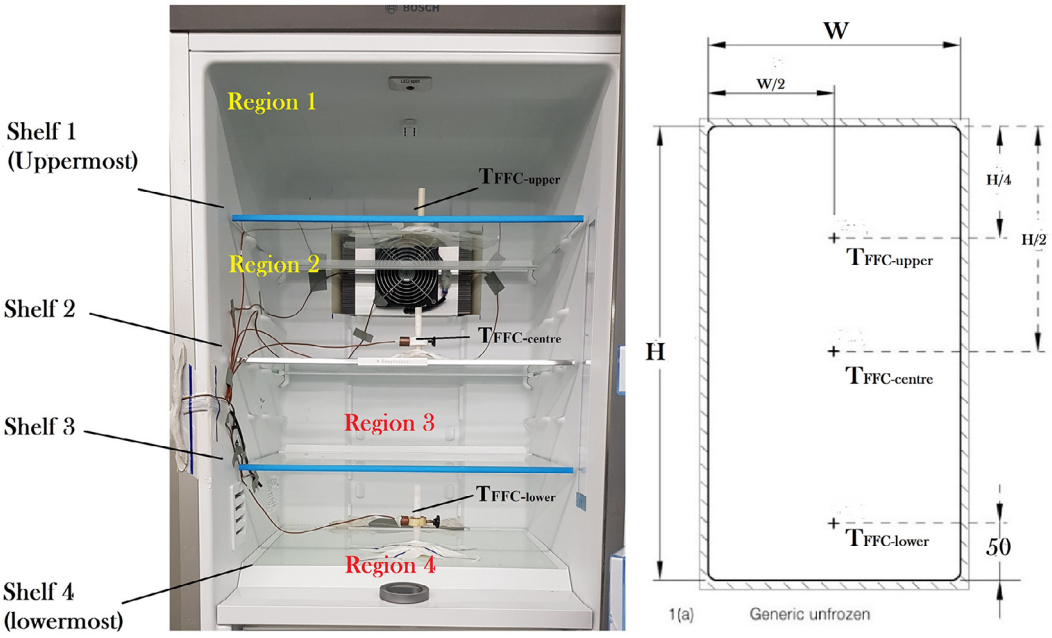


Fig. 2. The locations of temperature sensors.

Table 1
Sensors employed and their accuracy.

Measurement Value	Sensor	Measurement Range	Accuracy
Power	Zimmer LMG500	Voltage: 3–1000 V Current: 0.02–32 A	+/- 0.158W
Relative Humidity	Rotronic HF532, HC2S	0–100%rh	+/- 0.8%rh
Temperature	SAB (DIN EN 60,584)	−40 °C to +70 °C	+/- 0.2 °C
Air Velocity	Testo 425 Thermal Anemometer	0 to 20 m/s	+/- 0.01 m/s

fer. It has an operating temperature range varying from −10 °C to 60 °C. Its maximum cooling power is 143 W and operates at a DC voltage of 24 V. It was chosen in order to meet the cooling load needs of FFC. These requirements are based on the measurements of overall transmission losses and the calculations presented in former study (Söylemez et al., 2018).

2.3. Cooling time measurements

In order to measure cooling time of FFC, the "cooling capacity test" in the second part of IEC62552:2015 standard was taken into account. As stated, per 100 l of FFC volume, 4.5 kg of warm test packages (loads) need to be used and the time to bring packages' temperature from 25 °C to 10 °C shall be recorded. The test is performed in a climate chamber at an ambient temperature of 25.0 ± 0.5 °C and relative humidity of between 35 and 50% which comply with the requirements in the standard. For all target compartment temperatures, average air temperatures in each compartment are considered and their measured values shall not exceed the target compartment temperatures. For FFC, the target compartment temperature is +4.0 °C. During the tests, the refrigerator consumed an average power of 224.6 W.

In the examined compartment, there were three different temperature sensors located as presented in Fig. 2 (IEC-62552:2015, 2015). When determining temperature sensor positions inside the FFC, the dimensions of 695 × 495 × 515 mm for H x W x D were considered. The temperature sensors were inserted into the centre of Cu cylinders, made of brass or tin-covered copper with masses of 25 $g \pm 5\%$. The sensors used for the measurements and their accuracy are listed in Table 1. The accuracies for the power, relative humidity, and temperature measurements are at the desired level to meet requirements in the standard.

After the target compartment temperatures fulfilled the compliance criteria and reached the steady state, the warm packages were inserted into the FFC in the given order specified in IEC62552:2015 as presented in Fig. 3. There were 15 packages, in total 7.5 kg, which were evenly distributed to three shelves where temperature sensors were located, Shelf 1 (uppermost shelf), Shelf 2, and Shelf 4 (five packages on each shelf). On each shelf, two packages were M-packages; that is, the measurements were taken from these ones (shown with red colour in Fig. 3). The warm packages shall be at a temperature of 25.0 ± 0.5 °C prior to insertion.

The measurement data for power and voltage was collected by means of a network-based system, whereas the rest of the data such as temperature, relative humidity, and compressor and TEC run time was collected by data logger (Agilent 34970A). The power and voltage measurements were recorded in every 5 s, while the measurements for the rest in every 15 s and then processed through a software tool used in the BSH for data analysing. High accuracy instruments were used for the test. Relative humidity's overall accuracy was less than 5%. The temperatures inside the compartment and climate chamber (test room) were measured by T type thermocouples that have an uncertainty of ±0.2 °C. The packages used in the test have exactly the same chemical content

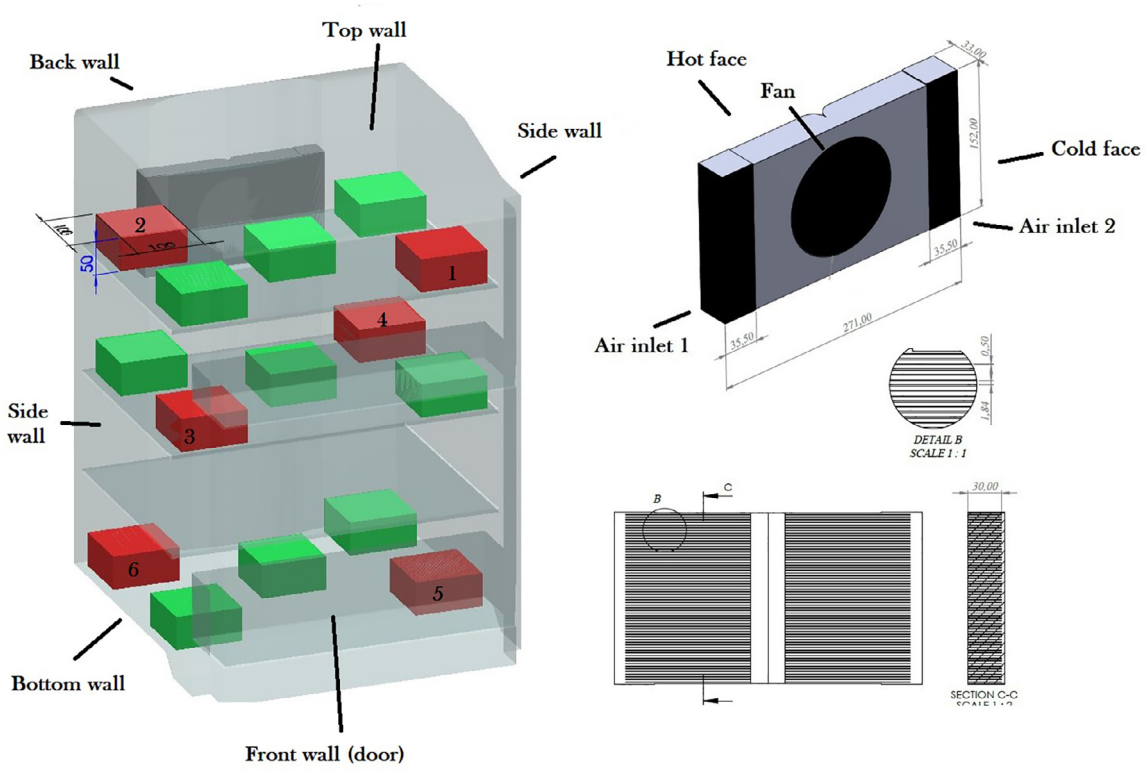


Fig. 3. Geometric model of the FFC.

defined in the standard. The tolerances for their dimensions and masses were ± 2 mm and ±2%, respectively. A thermal anemometer with ±0.5 °C accuracy and 0.01 ms^{-1} resolution was used for low air velocity measurements.

In order to obtain the cooling time performance, temperature readings for the packages were measured using the thermocouples described in the previous paragraph and they were recorded at every minute. An uncertainty analysis was performed for these temperature readings. For this purpose, temperature readings for each test package were repeated three times and the standard deviations of temperature readings at each minute were calculated in order to estimate the random error in the measurements. In addition to this, since the temperature sensors used for the measurements also had an uncertainty of ±0.2 °C, the total amount of uncertainty at each of the points was calculated by taking the square root of the sum of the squares of the random error and sensor uncertainty.

2.4. CFD analysis

In the context of this work, a simulation model was developed for predicting the cooling time of warm packages inserted into the FFC. To achieve this, the experimental tests were conducted in order to collect reference test data. Based on the testing data, CFD analyses were conducted considering three different turbulence models. ANSYS R18.1 FLUENT (ANSYS, 2020) was considered as simulation tool.

For the application in this work, several assumptions were made so as to simplify the problem. The air is incompressible (Mach number < 0.3). Flow is transient and inside the compartment turbulent flow occurs due to the forced convection. Boussinesq model is taken into consideration. The leakages through the gaskets of the door and the heat transfer by radiation are neglected.

2.4.1. Formulation for the analysis

Regarding the given assumptions above, three governing equations, Eqs. (1)-(3) were taken into consideration. These equations are mass, momentum, and energy conservation (Çengel, 2006).

- *Conservation of mass*

$$\nabla \cdot \vec{V} = 0 \tag{1}$$

- *Conservation of momentum*

$$\rho \frac{D\vec{V}}{Dt} = \rho\vec{g} - \nabla p + \mu \nabla^2 \vec{V} \tag{2}$$

In Eq. (2), μ is the effective viscosity coefficient including both dynamic (molecular) viscosity and eddy (turbulent) viscosity.

- *Conservation of energy*

The equation for energy conservation is based on the first law of thermodynamics, Eq. (3).

$$\rho c_p \frac{DT}{Dt} = k\nabla^2 T + \Phi \tag{3}$$

where, k is the effective thermal conductivity of the fluid, and Φ is the dissipation function.

2.4.2. Geometry of the model

The FFC geometry modelled via The ANSYS SpaceClaim for simulation is simpler than the original one in order to achieve the targets with less effort in terms of meshing and simulation time (ANSYS, 2020). The simplified geometry of the FFC (including TEC and packages) is demonstrated in Fig. 3.

The dimensions of the compartment, TEC, and packages are given in Table 2.

2.4.3. Details of mesh

The geometric model was meshed by means of ANSYS Meshing (ANSYS, 2020). Some of the properties' values are presented in Table 3. The initial values for mesh were selected. An unstructured grid of tetrahedron elements was built, which is shown in Fig. 4.

Table 2
The dimensions for geometric model.

Geometry	*H* [mm]	*W* [mm]	*D* [mm]	diameter [mm]
FFC	695	495	515	–
TEC cold face	152	271	33	–
Inlets	152	35.5	33	–
Fan	–	–	–	120
Packages	50	100	100	–

Table 3
Some of the values for the mesh.

Parameters	Values
Defaults	
Element order	Program controlled
Element size	5 mm
Sizing	
Growth rate	1.5
Maximum size	Default (10 mm)
Mesh defeaturing and size	Yes, 0.25865 mm
Minimum edge length	0.5 mm
Quality	
Smoothing	Medium
Inflation	
Inflation option	Smooth transition
Transition ratio	0.272
Maximum layers	5
Growth rate	1.2
Statistics	
Nodes	5381,398
Elements	3571,990

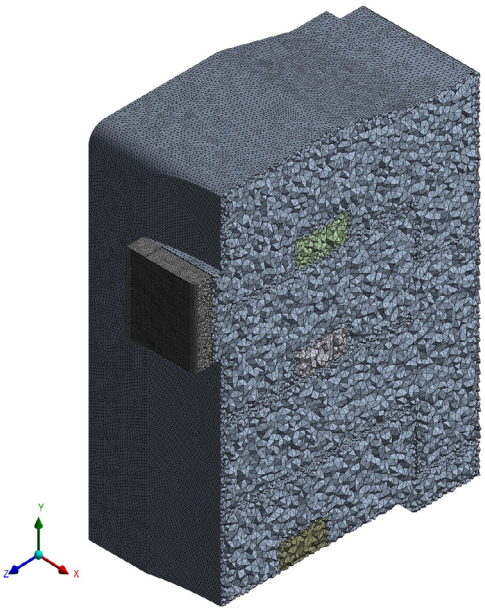


Fig. 4. Computational mesh.

2.4.4. Mesh quality

For the accurate predictions of the analysis, the quality of the mesh was also checked considering the element metrics of element quality, skewness, and aspect ratio. The values for them are presented in Fig. 5.

The average value for the element quality, which must be between 0 and 1, for this analysis was 0.828. It is almost ideal because the ideal value is 1 (ANSYS, 2020). The average skewness ratio shall be between 0 and 1. Meshing quality is said to be 'Excellent' if the skewness ratio is between 0 and 0.25 (ANSYS, 2020). In the analysis, its value was 0.24 that is excellent. Aspect ratio, which shall have reference values of 1 and ∞, has value of 1.86 that is relatively close to ideal value of 1 (ANSYS, 2020). It is clear that the quality of the mesh was at desired levels.

2.4.5. Numeric model

Flow was assumed to be fully turbulent and three different turbulence models were applied so as to find the most suitable one for the simulations. The models are standard k-ε, realizable k-ε, and transition SST.

2.4.6. Boundary conditions and materials

The locations of boundaries for TEC and FFC are demonstrated in Fig. 3 and the dimensions are given in Table 2. Additionally, the boundary conditions for the air inlets and the walls are also listed in Table 4. The average wall surface and ambient temperature measurements on the FFC were considered for temperature boundary conditions. The ambient temperature was 298.20 K (25.05 °C). However, around the hot face of the TEC (TEC wall) and on the sidewalls of FFC (due to the skin condensers) the measured temperatures were relatively higher. The temperature measurements inside the CC were considered for the bottom wall's surface and ambient temperature values. Before loading, the average temperature for the packages was 298.15 K (25.0 °C).

The information for the air inlets is based on the test data; hence, the boundary conditions for the air inlets are not symmetric although the model is geometrically symmetric. The inlet temperatures are almost the same while there is a difference in the average air velocities.

The convective heat coefficients (h) for the walls were calculated according to Eqs. (4)-(9) (Çengel, 2006).

$$h = \frac{Nuk}{L_c} \tag{4}$$

The values for k were collected from the measurements for overall transmission losses of the compartments as presented in Söylemez et al. (2018). The equations used in order to calculate Nu are:

The sidewalls, rear and front wall were assumed to be vertical plates (Çengel, 2006).

$$Nu = \left\{ 0.825 + \frac{0.387 {Ra_L}^{1/6}}{\left[1 + (0.492/\mathrm{Pr})^{9/16}\right]^{8/27}} \right\}^2 \tag{5}$$

The top wall was accepted as horizontal plate (Çengel, 2006).

$$Nu = 0.54 {Ra_L}^{1/4} \tag{6}$$

The bottom wall was also accepted as horizontal plate. However, because of having lower temperature value compared to top wall, Eq. (7) was used (Çengel, 2006).

$$Nu = 0.27 {Ra_L}^{1/4} \tag{7}$$

Where,

$$Ra_L = Gr_L \mathrm{Pr} = \frac{g\beta (T_s - T_\infty) {L_c}^3}{\nu^2} Pr \tag{8}$$

L_c is the height of the FFC for the side, rear, and front walls. For the top and bottom ones, it was

$$L_c = \frac{A_s}{P_s} \tag{9}$$

where A_s is the surface area and P_s is the perimeter.

In the calculations, for T_∞ value and for the temperature of outer surfaces (T_s) of the FFC walls, the temperature of the test chamber and the measured surface temperature values were considered, respectively. As mentioned earlier, owing to skin condensers in the side walls, the outer surface temperature of the side walls was relatively higher than those of the rest of the walls. The outer surface temperature of the bottom wall has the lowest temperature value due to being neighbour to CC.

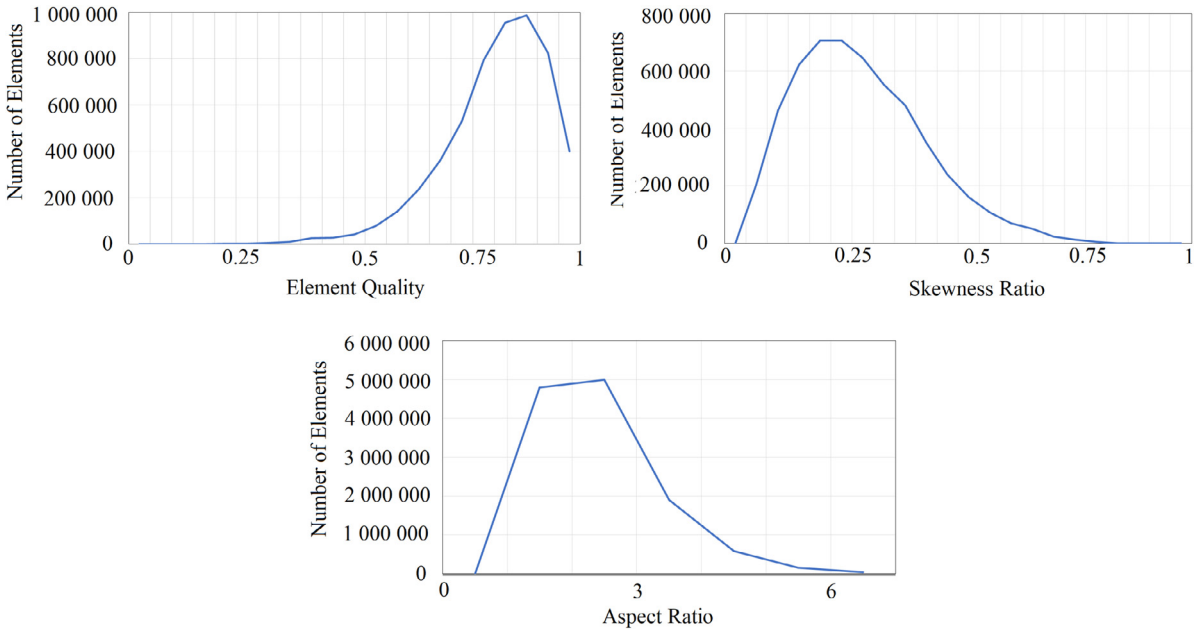


Fig. 5. Element metrics for mesh quality.

Table 4
Boundary conditions and materials.

Boundary	Thermal conditions	T_a [K]	h [$Wm^{-2}K^{-1}$]	v [ms^{-1}]	ρ [kgm^{-3}]	c_p [$Jkg^{-1}K^{-1}$]	k [$Wm^{-1}K^{-1}$]
Air inlet							
Inlet 1	–	274.4	–	2.10	–	–	–
Inlet 2	–	274.6	–	2.45	–	–	–
Walls							
Top wall	Convective	298.2	1.80	No slip	–	–	–
Side walls	Convective	305.7	2.91	No slip	–	–	–
Front wall	Convective	298.2	1.64	No slip	–	–	–
Back wall	Convective	298.2	2.15	No slip	–	–	–
Bottom wall	Convective	275.7	2.17	No slip	–	–	–
TEC							
TEC wall	Convective	300.1	16.37	No slip	–	–	–
Fluid							
Air	–	–	–	–	1.225	1006.43	0.0242
Solid							
Aluminium	–	–	–	–	2719	871	202.4
Expandable polystyrene	–	–	–	–	26.25	1200	0.0345
Polyurethane	–	–	–	–	34.5	1500	0.022
Vacuum insulated panel	–	–	–	–	225	1050	0.005
Packages	–	–	–	–	1000	3638.9	0.4

3. Results and discussion

3.1. Test results

According to IEC62552:2015 (IEC-62552:2015, 2015), the target mean temperature of warm M-packages (six packages in total) is 10 °C. It means some loads/packages are warmer than this value, whereas the rest are colder at the end period of cooling time. If the minimum microbial growth temperature of 5 °C is taken into account, all the loads are still in detrimental temperature range. Yet, there are different kind of microorganisms that are able to grow at different temperature levels, such as thermophiles (above 45 °C, best between 55 °C and 65 °C); mesophiles (between 20 °C and 45 °C); psychrophiles (−5 °C and 5 °C) (ASHRAE, 2014). If the psychrophiles are considered as reference, even cooling the foods to 5 °C will not be enough to keep them from spoilage. In Table 5, approximate minimum growth temperature values are given for some common organisms. It can be seen that several organisms' minimum growth temperature is 10 °C; hence, it is very beneficial to reduce the foods' temperature below this limit immediately.

The results of the test are demonstrated in Fig. 6. An uncertainty analysis was also performed for the measurements displayed in Fig. 6. For this purpose, temperature readings for each test package in Fig. 6 were repeated three times and the standard deviations of temperature readings at each minute were calculated in order to estimate the random error in the measurements. In addition to this, the temperature sensors used for the measurements had an uncertainty of ±0.2 °C. Then the total amount of uncertainty at each of the points shown in Fig. 6 was calculated by taking the square root of the sum of the squares of the random error and sensor uncertainty. The error bars shown in Fig. 6 are added according to the time averaged value of the total uncertainty for each package. Here, the time averaged uncertainty for packages 1, 2, 3, 4, 5, 6 were calculated to be 0.0861%, 0.1675%, 0.0937%, 0.1336%, 0.0931%, 0.0916%, respectively. The cooling time was measured as 146.5 min (2.44 h). This result is very promising when compared to that of the commercial one's results (Söylemez et al., 2018).

Table 5
Minimum growth temperatures for some bacteria types in food products (ASHRAE, 2014).

Organism	Possible Significance	Approximate Minimum Growth Temperature, °C
Staphylococcus aureus	Foodbome disease	10
Salmonella spp.	Foodbome disease	5.5
Clostridium botulinum,	Foodbome disease	
proteolytic		10
nonproteolytic		3.3
Lactobacillus and Leuconostoc	Spoilage of fresh and cured meats	0
Listeria monocytogenes	Foodbome disease	1
Acinetobacter spp.	Spoilage of precooked foods	−1
Pseudomonads	Spoilage of raw fish, meats, poultry, and dairy products	−1

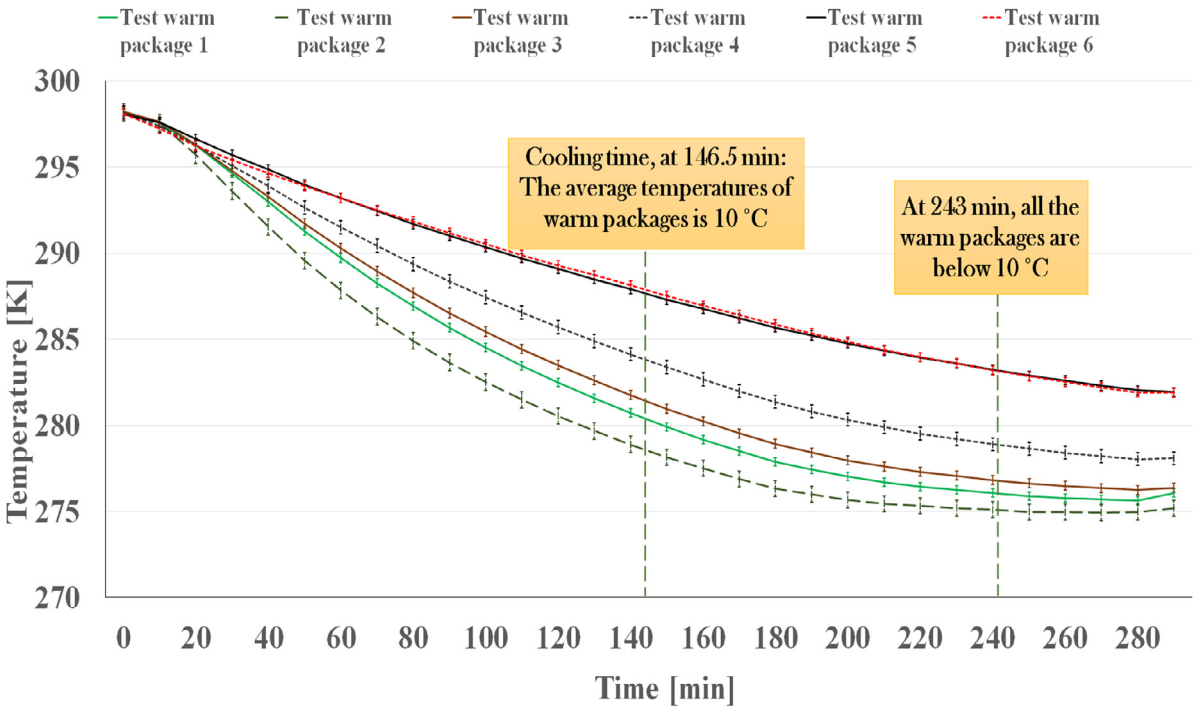


Fig. 6. Cooling time of each M-packages.

The packages close to the TEC (Warm package 1–2), which are located on the uppermost shelf, became cold faster and their temperatures dropped below the limit of 283.15 K (10 °C) in 2 h. At 243 min (≈4 h), all packages were below this limit. It can be recommended that sensitive foods to temperature should be kept at uppermost shelf.

3.2. CFD predictions

For the simulation work, a commercial workstation of DELL with 24 cores and 193 GB RAM was used. The total prediction time was around a week. The residuals for the governing equations are shown in Fig. 7. According to this figure, the residuals do not really go to zero, which indicates the unsteady nature of the flow inside the FFC.

The instantaneous temperature values of the M-packages at the end of cooling time of the test and the predictions are shown in Table 6. The uncertainty values shown in this table are added for the measurements according to the total uncertainty calculations described above. Here, the uncertainty values added were not time averaged values, but they correspond to the reading shown in Table 6. Also, in this table, the percent relative error values shown were calculated by dividing the difference between the final temperature values of measurements and CFD predictions by the difference between the initial and final temperature values of the measurements (actual amount of cooling). Then the result is multiplied by 100.

It is seen from the Table 6 that the CFD predictions of all models for the packages near the TEC, especially the ones on the uppermost and mid shelves (Warm package 1–4), are in good agreement with the measurement results; since, the maximum temperature difference is 1.9 K (below 10%). Nevertheless, the predictions for the packages (Warm package 5–6) on the lowermost shelf deviate from the measurement results. The maximum deviation is seen in the predictions for the cooling of Warm package 5. The highest deviation is by 7.5 K (around 70%) when standard k-ε model is applied. Transition SST model performs well with a maximum deviation of 4.9 K. When the predictions of three viscous models are evaluated, the transition SST is slightly better than the k-ε models for the application considered in this work.

After insertion of the warm packages into the FFC, their temperature variations over cooling time for the measurement and transition SST model are presented in Fig. 8. First, it can be said that temperature curves are similar; that is, the curves for both the measurement and model have similar trends. The predictions for the Warm package 1–4 are reasonably close to the measurements. The best prediction is for the Warm package 4, because the curves for the measurement and the model almost

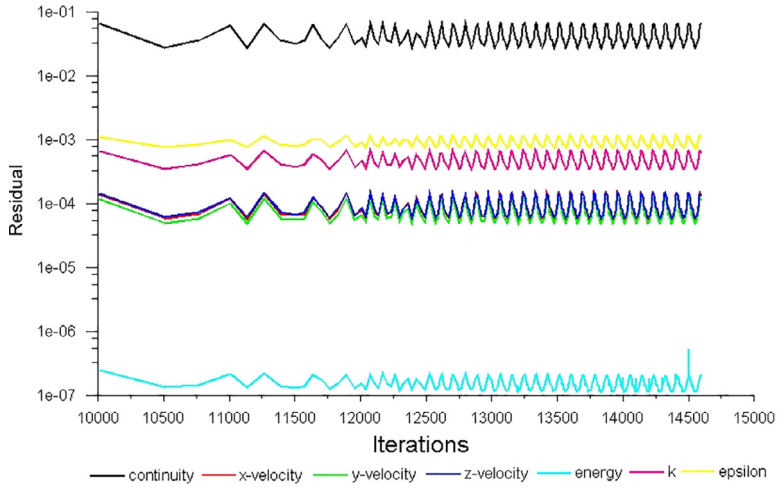


Fig. 7. Residuals of the governing equations.

Table 6
Comparison between CFD predictions and test result.

Viscous model&test	Warm package 1 *[K]*	Warm package 2 *[K]*	Warm package 3 *[K]*	Warm package 4 *[K]*	Warm package 5 *[K]*	Warm package 6 *[K]*
Measurement	280.3 ± 0.2	278.5 ± 0.9	281.3 ± 0.3	283.7 ± 0.7	287.6 ± 0.2	287.8 ± 0.2
Standard k-ε	280.6	280.4	282.3	283.4	295.1	293.8
Realizable k-ε	280.5	280.4	282.4	283.7	293.2	292.0
Transition SST	281.1	280.1	282.8	284.3	292.4	291.6
Standard k-ε	1.6%	9.6%	5.6%	−2.4%	70.8%	58.3%
Realizable k-ε	1.5%	9.5%	6.1%	−0.1%	53.4%	40.8%
Transition SST	4.5%	8.0%	8.6%	4.1%	46.1%	37.3%

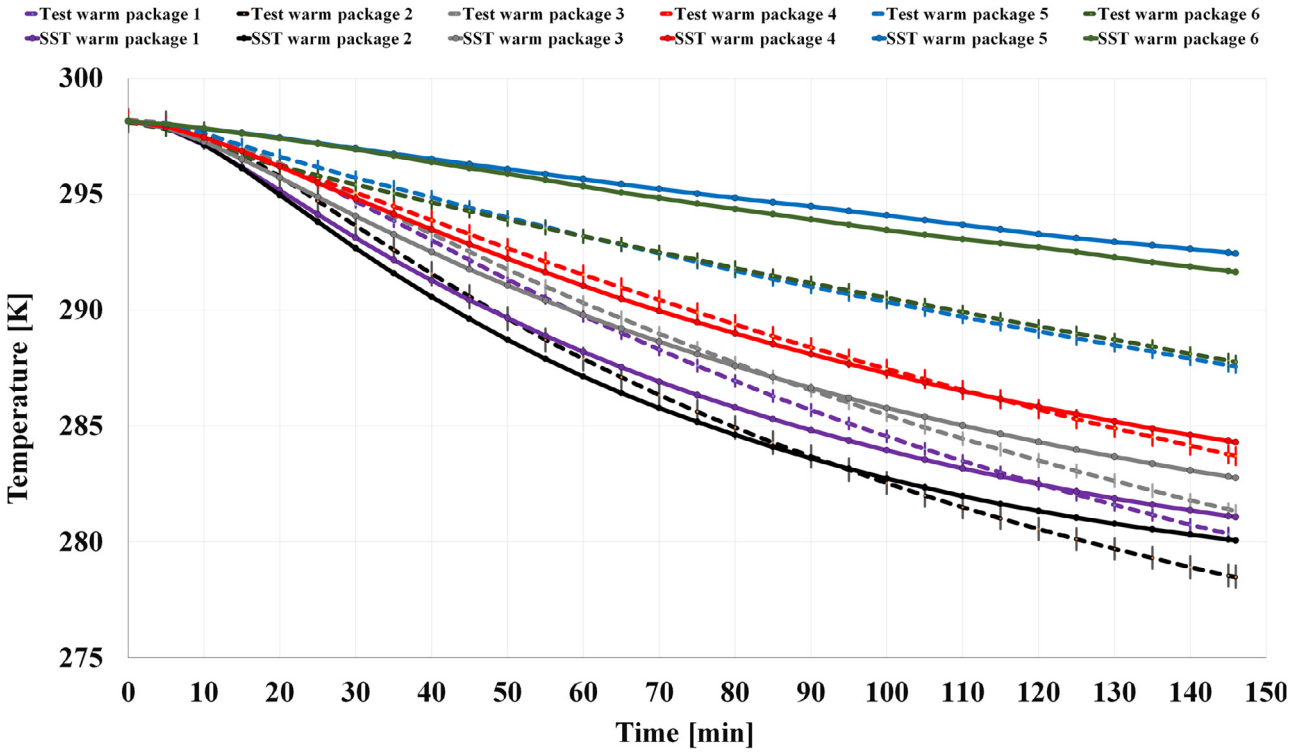


Fig. 8. Cooling times of the packages for measurement and transition SST model.

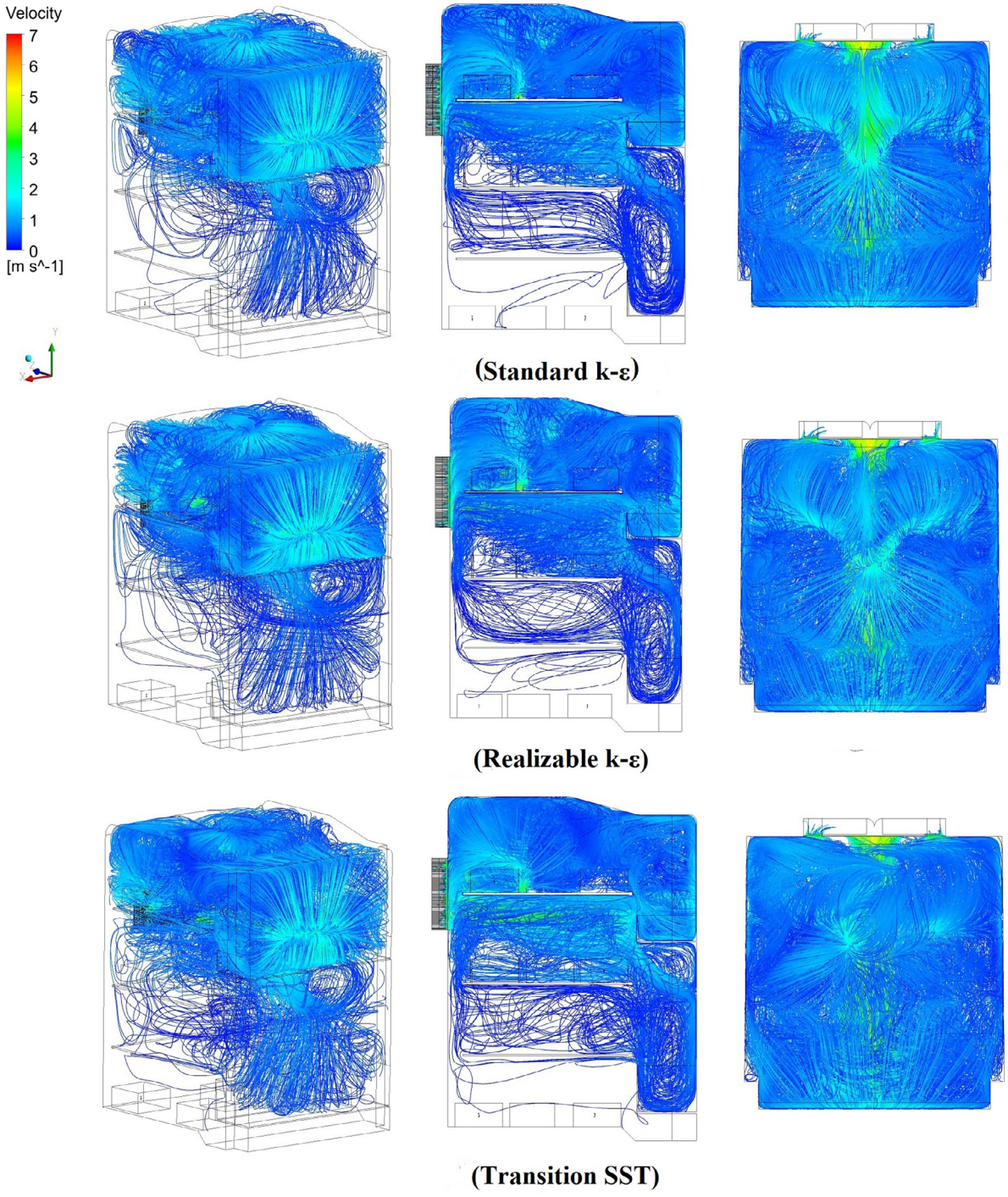


Fig. 9. Air velocity distribution inside the FFC.

match during the whole cooling period. However, the deviation is higher for the predictions of Warm package 5–6 in the given period.

In Figs. 9 and 10, air velocity and temperature distribution inside the FFC are shown, respectively. In Fig. 9, dark blue streamlines represent the cold air supplied by the TEC via air inlets while the other colors represent the warmer air sucked by the TEC fan. The regions, where streamlines are dense, get very airy. In regions where the air is sparse, the flow rate is low. In Fig. 10, a temperature stratification inside the compartment can be seen. The upper region is colder (represented with blue) than the bottom region. According to these figures, cold air intensifies in Region 1–2 and consequently these two regions are colder than the rest of them. This explains rapid cooling of warm packages located on the Shelf 1–2. The least cold air moves to Region 4 leading to warmer temperature levels in this region. For Region 4, transition SST's predictions are much better than the others due to the fact that cold air reaches the packages positioned on the lowermost shelf (Shelf 4) and cools the warm packages faster. Owing to this, the prediction results of the transition SST model are closer to the measurement results for the Warm packages 5–6.

The differences in the prediction accuracies of warm packages' cooling are mainly due to heat convection behaviours in the regions. The TEC is mounted to the back wall between the Region

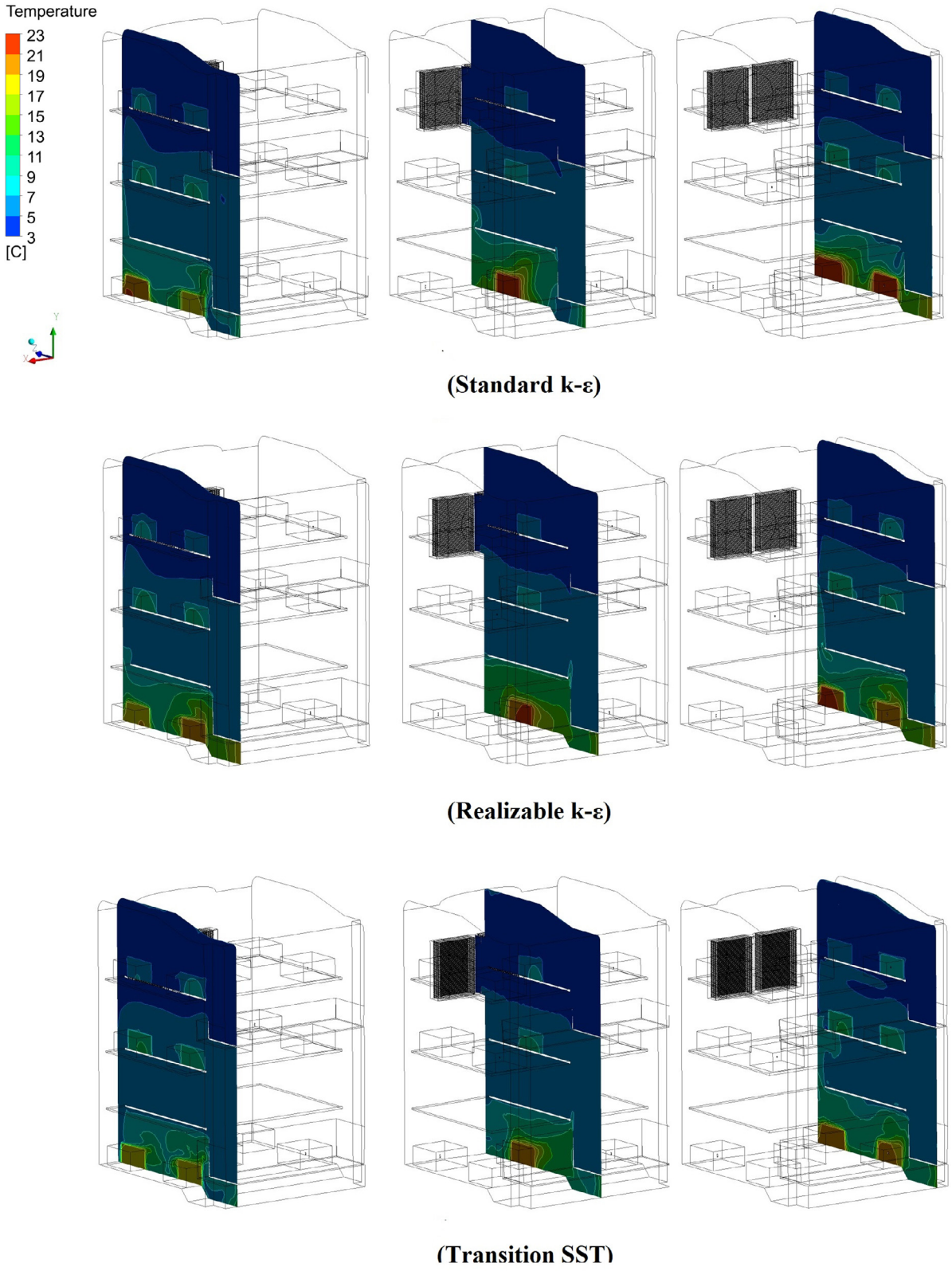


Fig. 10. Temperature distribution inside the FFC.

1–2 and the cold air velocities are higher, which create forced convection and strong airflow characteristics. Therefore, the CFD predictions are more accurate compared to the ones obtained for the packages in Region 4 in where there are weak airflows because of lower air velocities and therefore natural convection most likely occurs in these regions.

Finally, it can be said that the predicted air velocity and temperature distribution have similar patterns for all turbulence models. As seen from Fig. 10, there are tenuous differences between temperature fields' predictions of the models; however, Region 4 is predicted to be colder in transition SST's compared to other turbulence models.

Conclusions and future work

In this current work, a simulation study was conducted through CFD analysis to predict cooling time for the FFC of a domestic refrigerator cooled by TEC. Three different viscous models, standard k-ε, realizable k-ε, and transition SST, were compared in order to find the most suitable one to the test results. The tests were based on the "cooling capacity test" mentioned in IEC62552:2015.

The cooling time was measured as 146.5 min (2.44 h), which is lower than that of the commercial one's results. The packages close to the TEC (Warm package 1–2), which are located on the uppermost shelf, became cold faster and their temperatures dropped below the limit of 283.15 K (10 °C) in 2 h. It should be noted that temperature-sensitive perishable foodstuffs must be stored at uppermost shelf.

Concerning CFD predictions, it should be noted that there are no significant changes between the predictions of the given turbulence models, but the transition SST model predicts Region 4 where there is tenuous cold airflow more accurately. Eventually, it can be beneficial to use this model in similar applications. Furthermore, the predictions for the packages located in the uppermost regions (Region 1–2) are in good agreement with the measurements, below 10%, whereas the deviation is much higher, between 37% and 71%, for the predictions of the ones positioned in the bottommost region (Region 4) of the compartment in the given period. In this study, forced convection was assumed to occur between the packages and the air circulating inside the FFC. However, as it was mentioned before the air circulated around the packages in the lower region at very low velocities such that heat transfer can be thought to be more like free convection than forced convection. As a result, the discrepancy between numerical and experimental results for these packages was relatively high. In order to remedy this problem free convection model might be employed along with the forced convection model as a future work. In addition to this, using CFD methodology, finding the optimum position of TEC for the best cooling performance is also considered as a future work.

Declaration of Competing Interest

The authors declare that they have no known competing financial interests or personal relationships that could have appeared to influence the work reported in this paper.

Acknowledgments

Authors thank BSH Bosch R&D Centre of Refrigeration for providing test chambers and measurement instruments.

Supplementary materials

Supplementary material associated with this article can be found, in the online version, at doi:10.1016/j.ijrefrig.2020.11.012.

References

Alfaro-Ayala, J.Arturo, Uribe-Ramírez, Agustín R., Minchaca-Mojica, J.Isaac, Ramírez-Minguela, J.de J., Alvarado-Alcalá, B.Uciel, Lopez-Núñez, Oscar A., 2017. Numerical prediction of the unsteady temperature distribution in a cooling cabinet. Int. J. Refrig. 73, 235–245 Volume.

Ansys, I., 2020. Ansys R18.1 Fluent. ANSYS, Inc, Canonsburg.

António, C.C., Afonso, C., 2011. Air temperature fields inside refrigeration cabins: a comparison of results from CFD and ANN modelling. Appl. Therm. Eng. 31, 1244 Volumee1251.

ASHRAE, 2014. Ashrae Handbook Refrigeration. Ashrae, Atlanta SI edition ed..

Bayer, O., Oskay, R., Paksoy, A., Aradag, S., 2013. CFD simulations and reduced order modeling of a refrigerator compartment including radiation effects. Energy Convers. Manage. 69, 68–76 Volume.

Belman-Flores, J., Gallegos-Muñoz, A., 2016. Analysis of the flow and temperature distribution inside the compartment of a small refrigerator. Appl. Therm. Eng. 106, 743–752 Volume.

Belman-Flores, J., Gallegos-Muñoz, A., Puente-Delgado, A., 2014. Analysis of the temperature stratification of a no-frost domestic refrigerator with bottom mount configuration. Appl. Therm. Eng. 65, 299–307 Volume.

Çengel, Y.A., 2006. Heat and Mass Transfer A Practical Approach, 3rd edition McGraw-Hill, Singapore.

Ding, G.-.L., Qiao, H.-.T., Lu, Z.-.L., 2004. Ways to improve thermal uniformity inside a refrigerator. Appl. Therm. Eng. 24, 1827–1840 Volume.

Fukuyo, K., Tanaami, T., Ashida, H., 2003. Thermal uniformity and rapid cooling inside refrigerators. Int. J. Refrig. 26, 249–255 Volume.

Gupta, J., Gopal, M.R., Chakraborty, S., 2007. Modeling of a domestic frost-free refrigerator. Int. J. Refrig. 30, 311–322 Volume.

IEC-62552:2015, 2015. IEC 62552:2015 Household Refrigerating Appliances - Characteristics and Test Methods. International Electrotechnical Commission (IEC) s.l.:.

Laguerre, O., Amara, S.B., Moureh, J., Flick, D., 2007. Numerical simulation of air flow and heat transfer in domestic refrigerators. J. Food Eng. 81, 144–156 Volume.

Laguerre, O., Benamara, S., Flick, D., 2010. Numerical simulation of simultaneous heat and moisture transfer in a domestic refrigerator. Int. J. Refrig. 33, 1425–1433 Volume.

Laguerre, O., Benamara, S., Remy, D., Flick, D., 2009. Experimental and numerical study of heat and moisture transfers by natural convection in a cavity filled with solid obstacles. Int. J. Heat Mass Transf. 52, 5691–5700 Volume.

Li, Z., Zeng, X., Zhao, D., Ding, G., 2019. Schemes and effects on improvement of temperature uniformity inside indirect cooling wine cabinet. Appl. Therm. Eng. 157 (113723).

Nikitin, M.N., 2020. Numerical analysis of refrigerated display designs in terms of cooling efficiency. Int. J. Therm. Sci. 148 (106157).

Söylemez, E., Alpman, E., Onat, A., 2018. Experimental analysis of hybrid household refrigerators including thermoelectric and vapour compression cooling systems. Int. J. Refrig. 95, 93–107 Volume.

Söylemez, E., Alpman, E., Onat, A., Yükselentürk, Y., Hartomacıoğlu, S., 2019. Numerical (CFD) and experimental analysis of hybrid household refrigerator including thermoelectric and vapour compression cooling systems. Int. J. Refrig. 99, 300–315 Volume.

Zhang, C., Lian, Y., 2014. Conjugate heat transfer analysis using a simplified household refrigerator model. Int. J. Refrig. 45, 210–222 Volume.